

## A new quinoline-based fluorescent-colorimetric sensitive and selective chemosensor for "On-Off" Pb<sup>2+</sup> ion detection

Vanshika Sharma<sup>a</sup>, Srishti Dutta<sup>a</sup>, Devanand Sahu<sup>a</sup>, Abhilash Pandey<sup>a</sup>,  
Dishen Kumar<sup>a</sup>, Sanchita Das<sup>b</sup> and Goutam Kumar Patra<sup>a\*</sup>

<sup>a</sup>Department of Chemistry, Guru Ghasidas Vishwavidyalaya, Bilaspur, C.G, India

<sup>b</sup>Department of Chemistry, National Institute of Technology, Rourkela, Odisha, India

### Experimental

#### General information

##### 2.9 Competition with other metal ions

After dissolving **L** (2.47 mg, 0.01 mmol) in the solvent mixture (10 mL) that was previously indicated, 30 μL of the mixture was used to dilute it to 3 mL, resulting in a final concentration of 10 μM. Ten millilitres of triple-distilled water were used to dissolve them, together with M(NO<sub>3</sub>)<sub>x</sub> (0.1 mmol) and Pb(NO<sub>3</sub>)<sub>2</sub> (33.1, 0.1 mmol). To obtain ten equivalents of metal ions, three millilitres of receptor **L** (10 μM) solution were combined with thirty microlitres of each metal solution (10 mM). Next, to create 10 equivalents, 30 μL of Pb<sup>2+</sup> solution (10 mM) was added to the mixture of each metal ion and **L**. Room temperature UV-Vis and fluorescence spectra were obtained following a brief mixing period.

##### 2.10 Computational details

The program package GAUSSIAN-09 Revision C.01 was used for all calculations.<sup>1</sup> The hybrid exchange correlation functional, which uses the gradient-corrected DFT level and the Coulomb-attenuating technique B3LYP, was applied to fully optimise the Ligand's (**L**) gas phase geometries in the singlet ground state without requiring any symmetry.<sup>2</sup> It was found that the basis set 6-31++G was appropriate for all of the molecules. The form of the **L**+Pb<sup>2+</sup> complex (**1**) was optimised with LanL2DZ basis sets.

##### 2.11 Molecular Electrostatic Potential

The molecular electrostatic potential at any given place surrounding a molecule can be described by the complete charge distribution of the molecule and its relationship to the dipole moments. It offers insight into electron density that is useful in determining electrophilic reactivity, nucleophilic reactivity, and hydrogen-bonding interactions.<sup>3,4</sup>

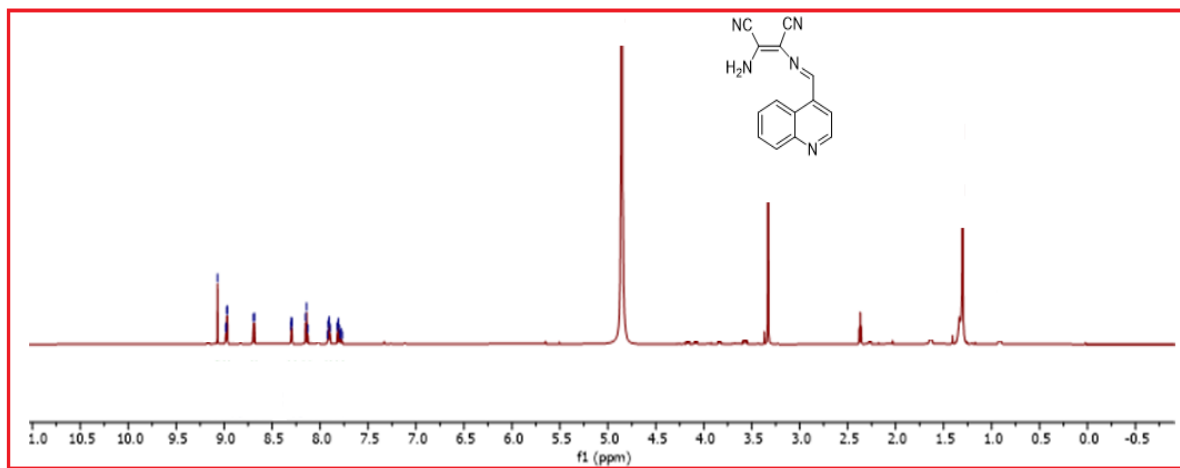


**Fig. S1.** <sup>1</sup>H NMR spectra of L in CD<sub>3</sub>OD.

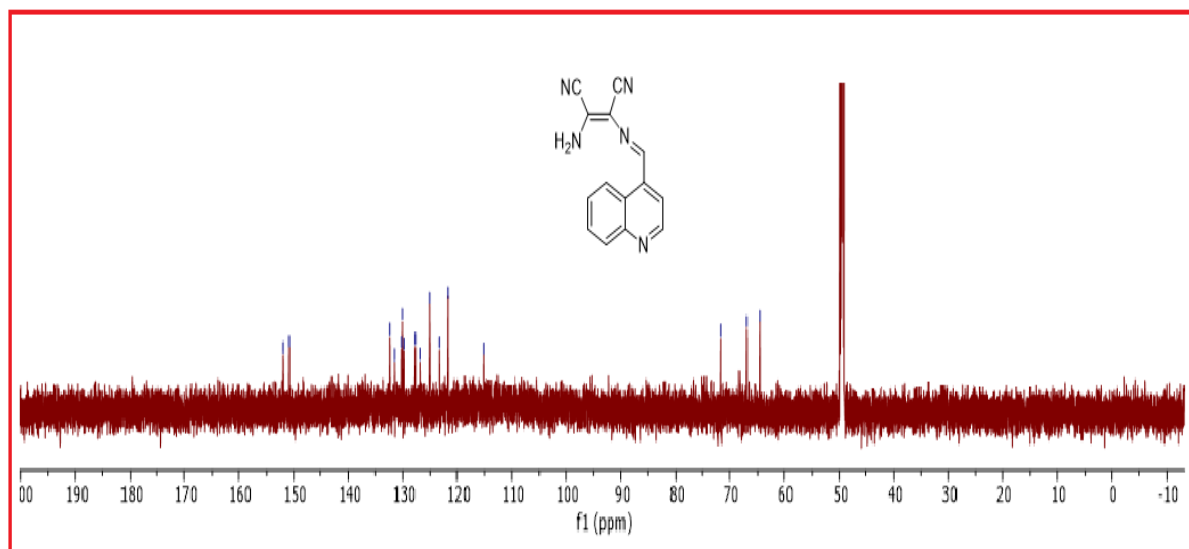


**Fig. S2.** <sup>13</sup>C NMR spectra of L in CD<sub>3</sub>OD.

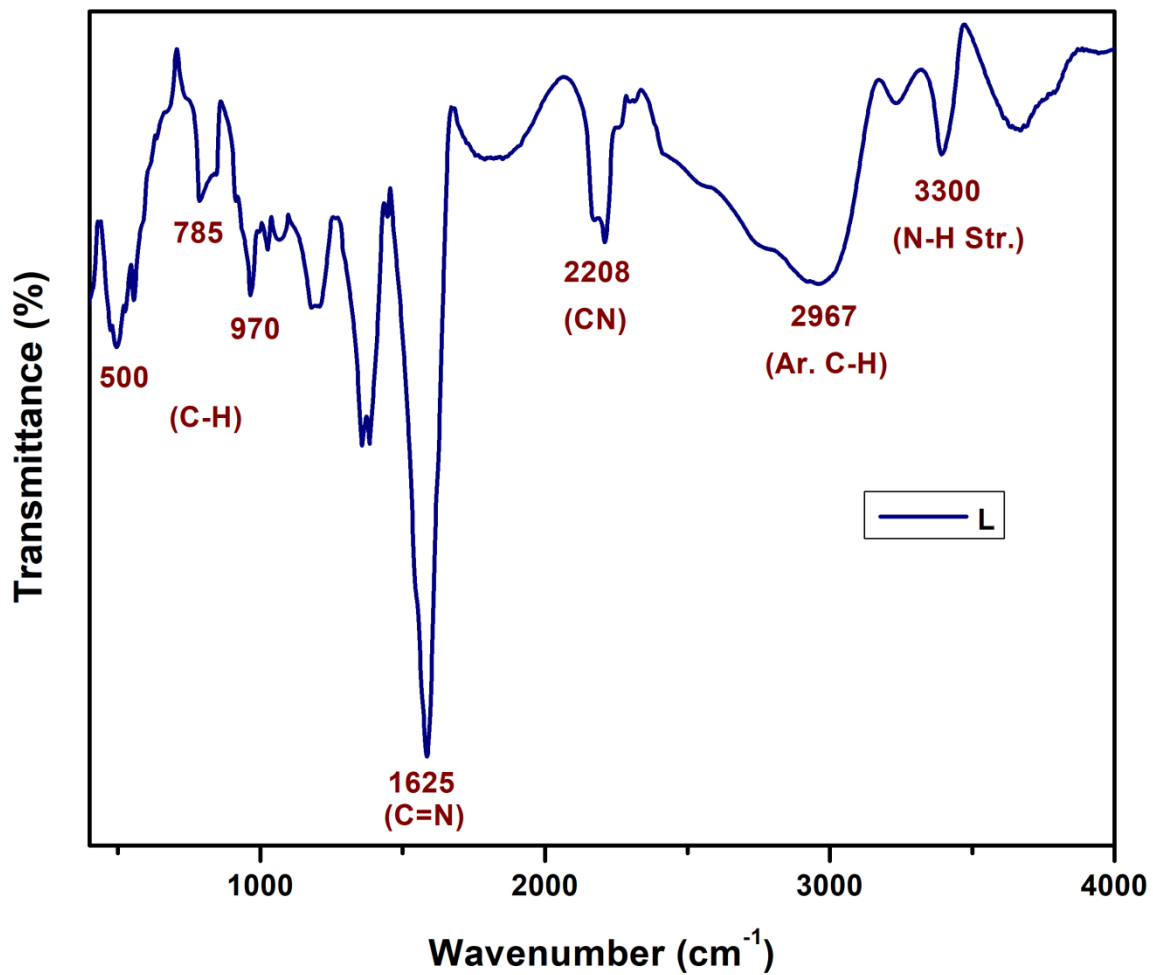


Fig. S3. FTIR spectra of L

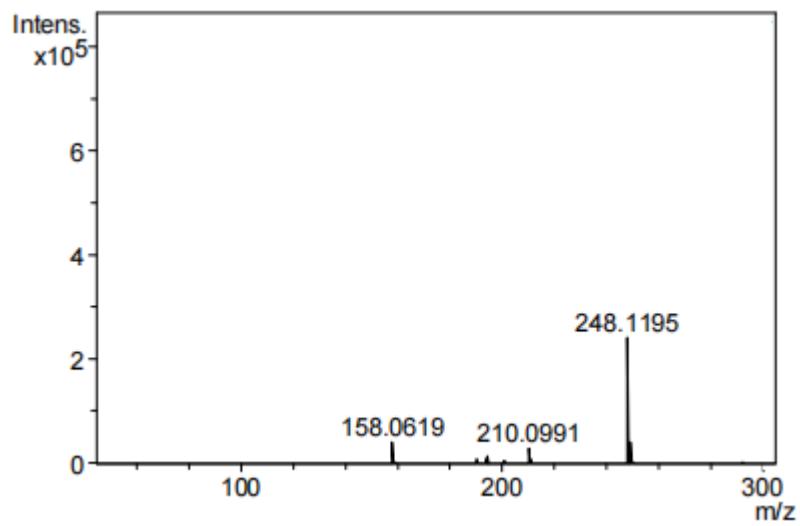


Fig. S4. ESI-mass spectra of L

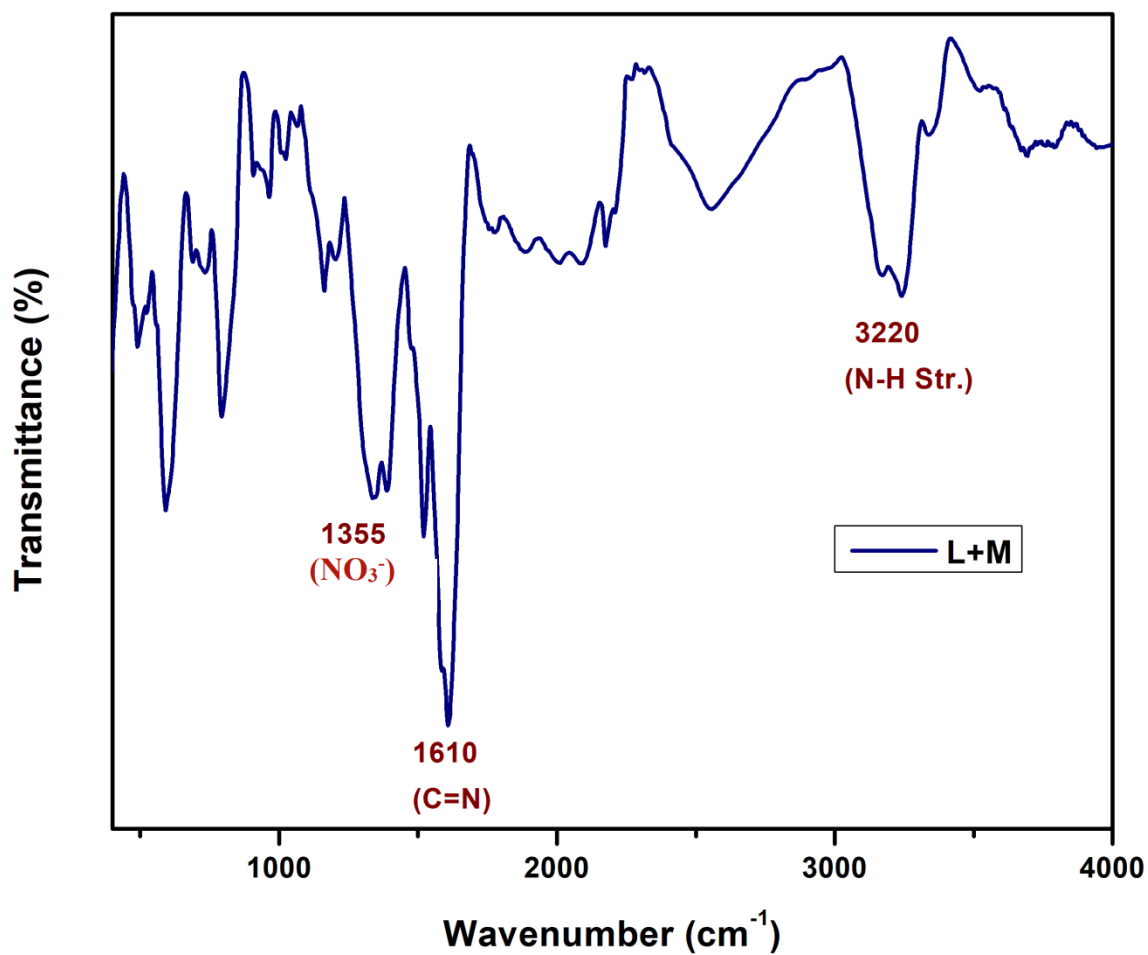


Fig. S5. FTIR spectra of L-Pb<sup>2+</sup> (1)

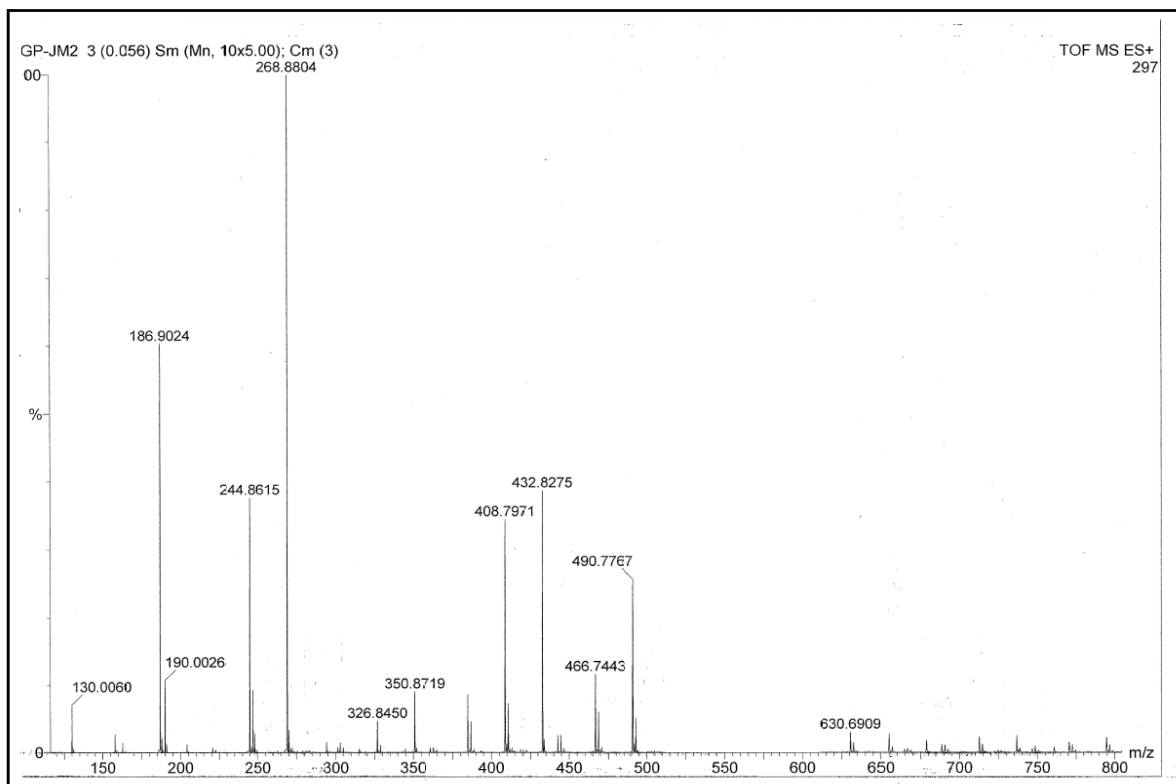


Fig. S6. ESI-mass spectra of L-Pb<sup>2+</sup> (1)

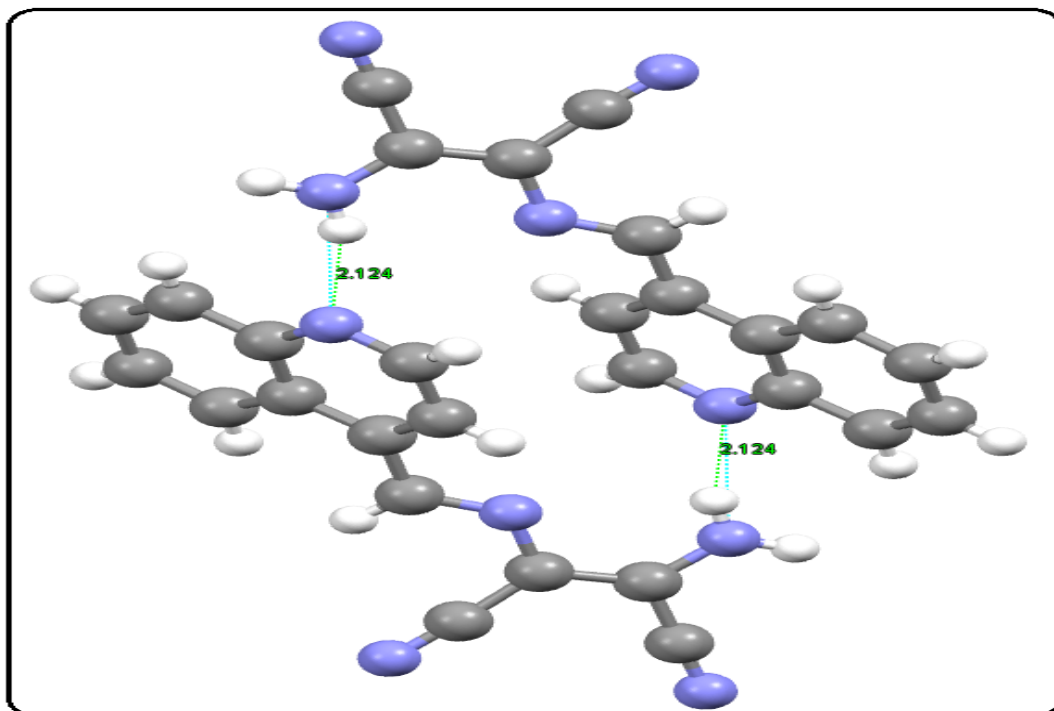


Fig. S7. Dimeric view of hydrogen-bonded L.

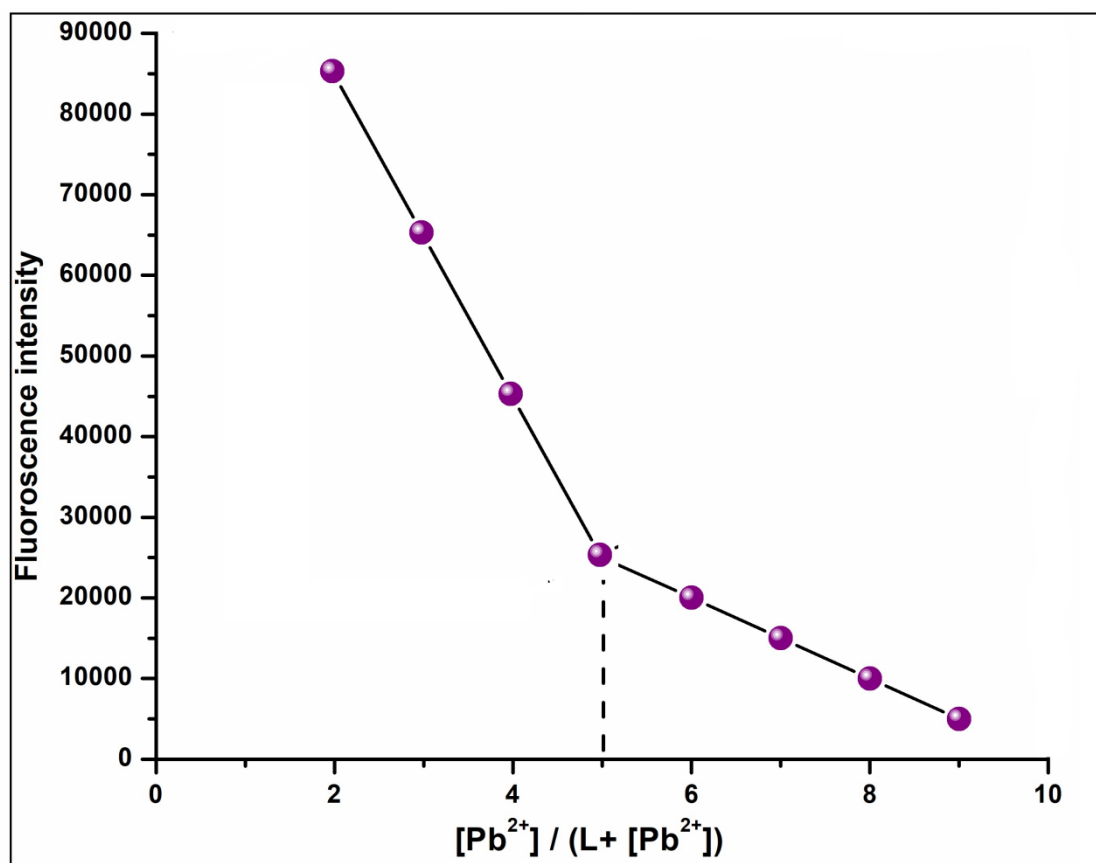


Fig. S8. Job's plot of L.

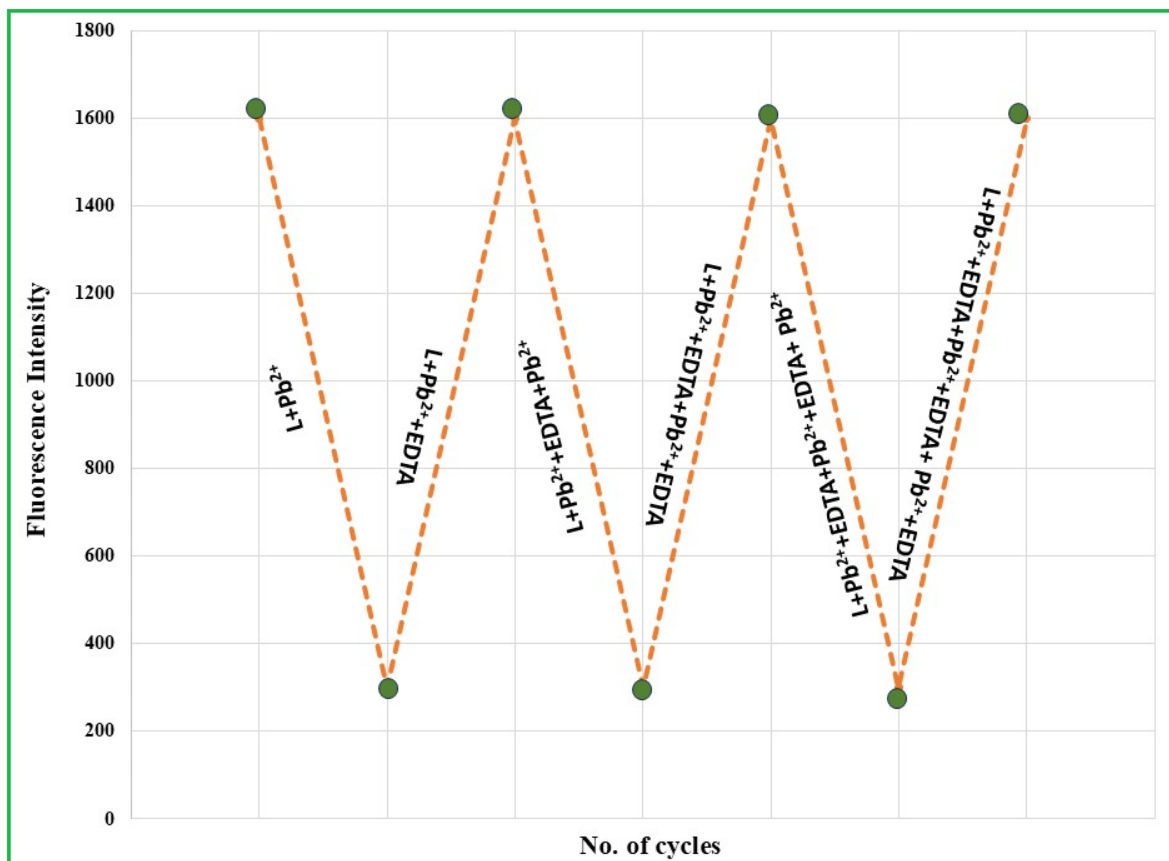


Fig. S9. Reversible cycle of L.

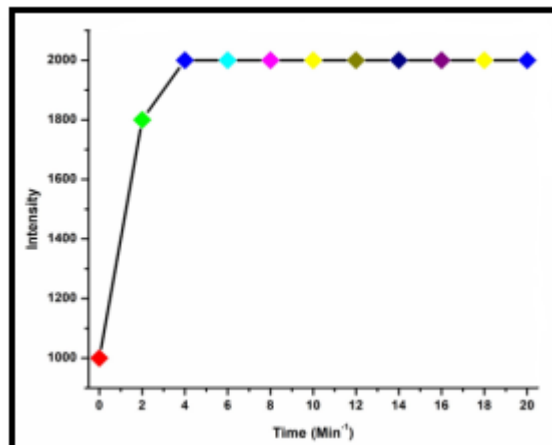


Fig. S10. Time-dependant fluorescence plot of L

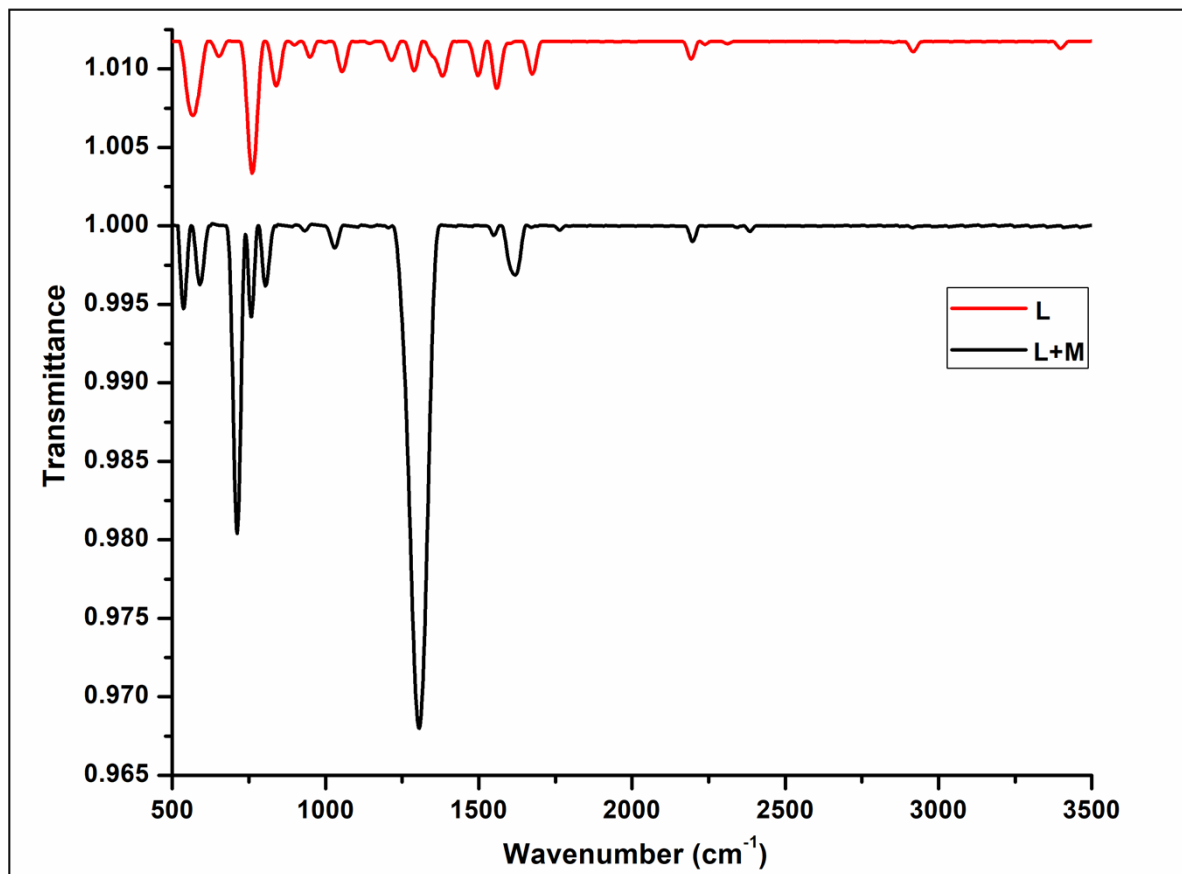


Fig. S11. Stag plot of the FTIR spectra of L and L-Pb<sup>2+</sup>

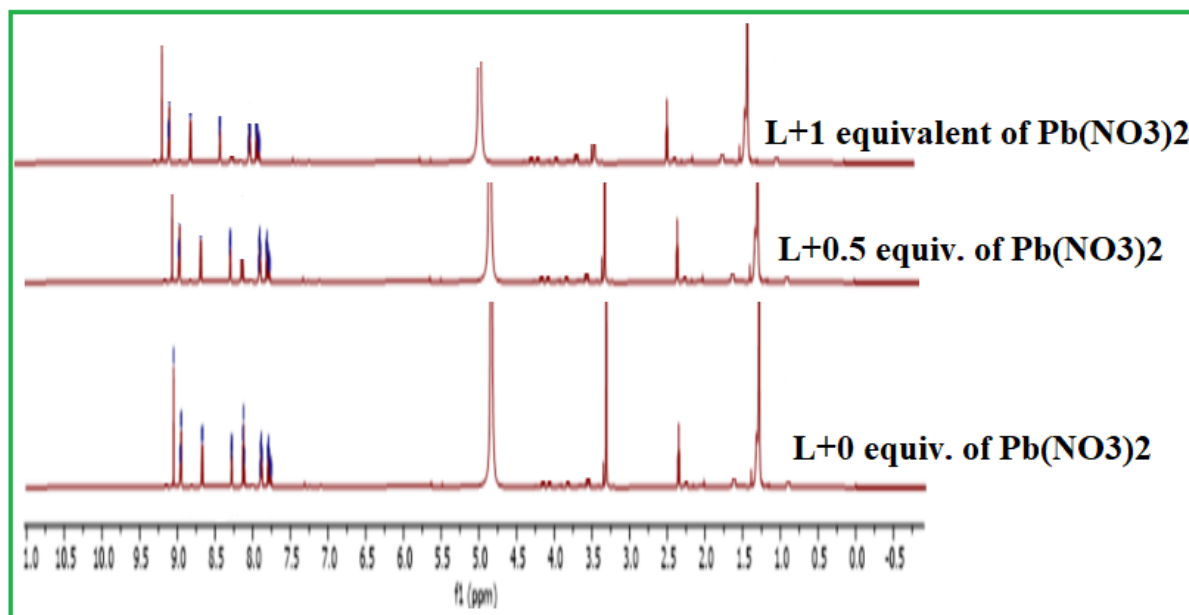


Fig. S12. The <sup>1</sup>H-NMR titration of L with Pb<sup>2+</sup>

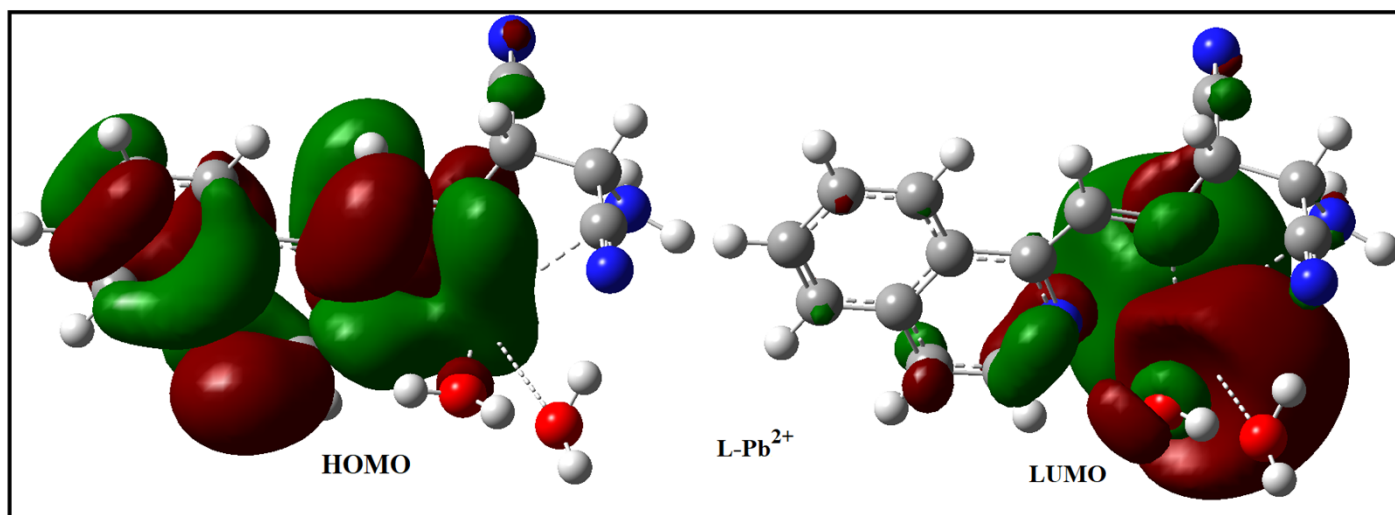


Fig. 13. The contour diagrams of HOMO and LUMO of L-Pb<sup>2+</sup>

Table S1. Bond Lengths for L

Atom	Atom	Length/Å	Atom	Atom	Length/Å
N001	C008	1.3951 (14)	C006	C00D	1.4142 (17)
N001	C009	1.2765 (15)	C007	C008	1.3703 (17)
N002	C006	1.3691 (16)	C007	C00G	1.4433 (17)
N002	C00C	1.3167 (16)	C008	C00F	1.4311 (17)
N003	C007	1.3339 (15)	C00A	C00C	1.3958 (17)
C004	C005	1.4289 (16)	N00B	C00F	1.1438 (16)
C004	C006	1.4194 (16)	C00D	C00I	1.355 (2)
C004	C00E	1.4149 (17)	C00E	C00J	1.3638 (18)
C005	C009	1.4701 (16)	C00G	N00H	1.1381 (16)
C005	C00A	1.3656 (17)	C00I	C00J	1.3974 (19)

TableS2. Bond Angles for L

Atom	Atom	Atom	Angle/°	Atom	Atom	Atom	Angle/°
C009	N001	C008	121.37 (10)	C008	C007	C00G	118.67 (11)
C00C	N002	C006	117.37 (10)	N001	C008	C00F	121.22 (10)
C006	C004	C005	117.32 (11)	C007	C008	N001	117.94 (10)
C00E	C004	C005	124.31 (11)	C007	C008	C00F	120.80 (10)



C00E	C004	C006	118.36 (11)	N001	C009	C005	119.70 (11)
C004	C005	C009	122.43 (10)	C005	C00A	C00C	120.28 (11)
C00A	C005	C004	118.19 (10)	N002	C00C	C00A	123.94 (12)
C00A	C005	C009	119.31 (11)	C00I	C00D	C006	120.36 (12)
N002	C006	C004	122.88 (10)	C00J	C00E	C004	120.35 (12)
N002	C006	C00D	117.70 (11)	N00B	C00F	C008	174.93 (13)
C00D	C006	C004	119.42 (11)	N00H	C00G	C007	178.94 (15)
N003	C007	C008	125.25 (11)	C00D	C00I	C00J	120.51 (12)
N003	C007	C00G	116.07 (11)	C00E	C00J	C00I	120.94 (13)

## References

1. M.J. Frisch, G.W. Trucks, H.B. Schlegel, G.E. Scuseria, M.A. Robb, J.R. Cheeseman, G. Scalmani, V. Barone, B. Mennucci, G.A. Petersson, H. Nakatsuji, M. Caricato, X. Li, H.P. Hratchian, A.F. Izmaylov, J. Bloino, G. Zheng, J.L. Sonnenberg, M. Hada, M. Ehara, K. Toyota, R. Fukuda, J. Hasegawa, M. Ishida, T. Nakajima, Y. Honda, O. Kitao, H. Nakai, T. Vreven, J.A. Montgomery, Jr., J.E. Peralta, F. Ogliaro, M. Bearpark, J.J. Heyd, E. Brothers, K.N. Kudin, V.N. Staroverov, R. Kobayashi, J. Normand, K. Raghavachari, A. Rendell, J.C. Burant, S.S. Iyengar, J. Tomasi, M. Cossi, N. Rega, J.M. Millam, M. Klene, J.E. Knox, J.B. Cross, V. Bakken, C. Adamo, J. Jaramillo, R. Gomperts, R.E. Stratmann, O. Yazyev, A.J. Austin, R. Cammi, C. Pomelli, J.W. Ochterski, R.L. Martin, K. Morokuma, V.G. Zakrzewski, G.A. Voth, P. Salvador, J.J. Dannenberg, S. Dapprich, A.D. Daniels, " O. Farkas, J.B. Foresman, J. V. Ortiz, J. Cioslowski, D.J. Fox, Gaussian 09, Revision C.01, Gaussian Inc., Wallingford, CT (2009).
2. A.D. Becke, *The Journal of Chemical Physics*, 1993, **98(7)**, 5648–5652.
3. S. Sebastian, N. Sundaraganesan, *Spectrochimica Acta Part A: Molecular and Biomolecular Spectroscopy*, 2010, **75(3)**, 941–952.
4. M. Rahimi, A. Amini, H. Behmadi, *Journal of Photochemistry and Photobiology A: Chemistry*, 2020, **388**, 112190.